COMPACTON-LIKE SOLUTIONS OF THE HYDRODYNAMIC SYSTEM DESCRIBING RELAXING MEDIA

V. A. VLADIMIROV

University of Science and Technology, Faculty of Applied Mathematics,
Al. Mickiewicza 30, 30-059 Krakow, Poland
(e-mail: vsan@rambler.ru)

(*Received September 20, 2007*)

We show the existence of a compacton-like solutions within the relaxing hydrodynamic-type model and perform numerical study of attracting features of these solutions.

Keywords: wave patterns, compactons, relaxing hydrodynamic-type model'

Mathematics Subject Classification: 35C99, 34C60, 74J35.

1. Introduction

In this paper there are studied solutions to evolutionary equations, describing wave patterns with compact support. Different kinds of wave patterns play the key rôle in natural processes. They occur in nonlinear transport phenomena (see [1] and references therein), serve as channels of information transfer in animate systems [2], and very often assure stability of some dynamical processes [3, 4].

One of the most advanced mathematical theory dealing with the formation of wave patterns and evolution is the soliton theory [5]. The origin of this theory goes back to Scott Russell's description of the solitary wave movement on the surface of channel filled with water. It was the ability of the wave to move quite a long distance without any change of shape which stroke the imagination of the first chronicler of this phenomenon. In 1895 Korteveg and de Vries proposed their famous equation

$$u_t + \beta\, u\, u_x + u_{xxx} = 0, \tag{1}$$

describing evolution of long waves on shallow water. They also obtained an analytical solution to this equation, corresponding to the solitary wave:

$$u = \frac{12\, a^2}{\beta}\, \mathrm{sech}^2\big[a(x - 4\, a^2\, t)\big]. \tag{2}$$

Both the already mentioned report by Scott Russell as well as the model suggested to explain his observation did not find a proper impact till the middle of 60-ies of the XX century when there was been established a number of outstanding features of Eq. (1) finally recognized aware as the consequences of its complete integrability [5].

In recent years there has been discovered another type of solitary waves referred to as *compactons* [6]. These solutions inherit main features of solitons, but differ from them in one point: their supports are compact.

A big progress is actually observed in studying compactons and their properties, yet most papers dealing with this subject are concerned with compactons as solutions to either completely integrable equations, or those which produce a completely integrable ones when reduced to a subset of traveling wave (TW) solutions [7, 8, 9].

In this paper the compacton-like solutions to the hydrodynamic-type model taking account of the effects of temporal nonlocality are studied. Being of dissipative type, this model is obviously non-Hamiltonian. As a consequence, compactons exist merely for selected values of the parameters. In spite of such restriction, the existence of these solutions in significant for they appear in the presence of relaxing effects and rather cannot exist in any local hydrodynamic model. Besides, the compacton-like solutions manifest attractive features and can be treated as some universal mechanism of the energy transfer in media with internal structure, leading to the given type of the hydrodynamic-type modeling system.

The structure of the paper is as follows. In Section 2 we give a geometric insight into the soliton and compacton TW solutions, revealing the mechanism of appearance of generalized solutions with compact supports. In Section 3 we introduce the modeling system and show that compacton-like solutions do exist among the set of TW solutions. In Section 4 we perform numerical investigations of the modeling system based on the Godunov method and show that the compacton-like solutions manifest attractive features.

2. Solitons and compactons from the geometric viewpoint

Let us discuss how the solitary wave solution to (1) can be obtained. Since the function $u(\cdot)$ in formula (2) depends on the specific combination of the independent variables, we can use for this purpose the ansatz $u(t,\, x) = U(\xi)$, with $\xi = x - V\,t$. Inserting this ansatz into Eq. (1) we get, after one integration, the following system of ODEs:

$$\begin{aligned} \dot{U}(\xi) &= -W(\xi), \\ \dot{W}(\xi) &= \frac{\beta}{2}\, U(\xi) \left(U(\xi) - \frac{2\,V}{\beta} \right). \end{aligned} \tag{3}$$

The system (3) is a Hamiltonian system described by the Hamilton function

$$H = \frac{1}{2} \left(W^2 + \frac{\beta}{3}\, U^3 - V\, U^2 \right). \tag{4}$$

So every solutions of (3) can be identified with some level curve $H = C$. As already mentioned the solution (2) corresponds to the value $C = 0$ and is represented by the homoclinic trajectory shown in Fig. 1 (the only trajectory in the right half-plane going through the origin). Since the origin is an equilibrium point of (3) and penetration of the homoclinic loop takes infinite “time”, then the beginning of this

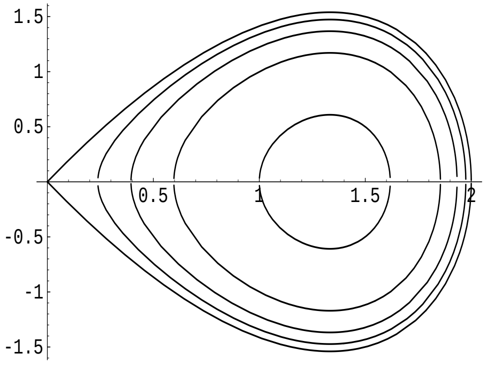

Fig. 1. Level curves of the Hamiltonian (4), representing periodic solutions and limiting to them homoclinic solution

trajectory corresponds to $\xi = -\infty$ while its end to $\xi = +\infty$. This assertion is equivalent to the statement that solution (2) is nonzero for all finite values of the argument ξ.

Now let us discuss the geometric structure of compactons. For this purpose we return to the original equation which is a nonlinear generalization of the classical Korteveg–de Vries equation [6],

$$u_t + \alpha \left(u^m\right)_x + \beta \left(u^n\right)_{xxx} = 0. \tag{5}$$

Like in the case of Eq. (1), we look for the TW solutions $u(t, x) = U(\xi)$, where $\xi = x - V t$. Inserting this ansatz into (5) we obtain, after one integration, the following dynamical system:

$$\frac{dU}{dT} = -n\,\beta\, U^{2\,(n-1)}\, W, \tag{6}$$
$$\frac{dW}{dT} = U^{n-1}\left[-V\,U + \alpha U^m + n\,(n-1)\,\beta\, U^{n-2} W^2\right],$$

where

$$\frac{d}{dT} = n\,\beta\, U^{2\,(n-1)}\,\frac{d}{d\xi}.$$

All the trajectories of this system are given by its first integral

$$U^{n-1}\left(\frac{n\,\beta}{2}\,U^{n-1}\,W^2 + \alpha\,\frac{U^{m+1}}{m+n} - \frac{V}{n+1}\,U^2\right) = H = \text{const.} \tag{7}$$

The phase portrait of system (6) shown in Fig. 2 is to some extent is similar to that corresponding to system (3). Yet the critical point $U = W = 0$ of the system (6) lies on the line of singular points $U = 0$. And this implies that modulus of the tangent vector field along the homoclinic trajectory is bounded from below by

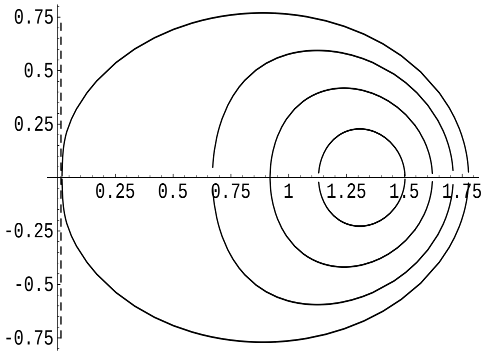

Fig. 2. Level curves of the Hamiltonian (7). Dashed line indicates the set of singular points $U = 0$.

a positive constant. Consequently the homoclinic trajectory is penetrated in a finite time and the corresponding generalized solution to the initial system (5) is the compound of a function corresponding to the homoclinic loop (which now has a compact support) and zero solution corresponding to the rest point $U = W = 0$. In case when $m = 2$, $\beta = 1/2$ and $n = 2$ such solution has the following analytical representation [6]:

$$u = \begin{cases} \dfrac{8\,V}{3\,\alpha}\cos^2\sqrt{\dfrac{\alpha}{4}}\,\xi & \text{when } |\xi| < \dfrac{\pi}{\sqrt{\alpha}}, \\ 0 & \text{when } |\xi| \geq \dfrac{\pi}{\sqrt{\alpha}}. \end{cases} \tag{8}$$

It is quite obvious that similar mechanism of creating the compacton-like solutions can be realized in case of non-Hamiltonian system as well, but, in contrast to the Hamiltonian systems, the homoclinic solution is no more expected to form a one-parameter family like this is the case with solution (8). In fact, in the considered modeling system the homoclinic solution appears as a result of a bifurcation following the birth of the limit cycle and its further interaction with the nearby saddle point.

Let us note in conclusion that we do not distinguish solutions having the compact supports and those which can be made so by proper change of variables. In particular, the solutions we deal with in the following sections, are realized as compact perturbations evolving in a self-similar mode on the background of the stationary inhomogeneous solution of the modeling system of PDEs.

3. Relaxing hydrodynamic-type model and its qualitative investigations

It is of common practice to use the concept of continual models when describing the wave processes in various media. This concept is well justified when the characteristic length λ of a wave packet is much larger than the characteristic size

d of the constituents of media. Usually this is the case in pure materials. But the situation is completely different when the wave packet propagates in materials possessing internal structure different from atomic one (such e.g. as soils, rocks or air-liquid mixtures). The description of intense pulse loading after action in such media could not be based on formalism of continuum mechanics, at least in its classical form. The model presented below corresponds to the situation when the ratio d/λ is such that continuum description is still valid, but the presence of internal structure should not be ignored. Asymptotic analysis shows [10] that the balance equations for the mass and momentum in the long wave approximation do not depend on the structure and retain their classical form. So all the information about the structure in this approximation should be contained in the constitutive equation which is necessary to make the system of the balance equations closed. Such constitutive equation for a medium with one relaxing process in the elements of structure was obtained in [11] by means of nonequilibrium thermodynamics methods. Together with the balance equations of momentum and mass it forms the following system:

$$\begin{aligned} u_t + p_x &= \gamma, \\ V_t - u_x &= 0, \\ \tau\, p_t + \frac{\chi}{V^2}\, u_x &= \frac{\kappa}{V} - p. \end{aligned} \tag{9}$$

Here u is mass velocity, V is specific volume, p is pressure, γ is acceleration of the external force, κ and χ/τ are squares of the equilibrium and “frozen” sound velocities, respectively, t is time, x is mass (Lagrangean) coordinate.

REMARK. Note that the last (constitutive) equation of the system (9) formally can be obtained from the nonlocal “flow-force” relation

$$p = \frac{\chi}{\tau\, V} - \sigma \int_{-\infty}^{t} e^{-\frac{t-t'}{\tau}}\, V^{-1}\left(t',\, x\right)\, d\,t'.$$

We perform the factorization [12] of the system (9) (or, in other words, passage to an ODE system describing TW solutions), using its symmetry properties summarized in the following statement.

LEMMA 1. *System* (9) *is invariant with respect to one-parameter groups of transformations generated by infinitesimal operators*

$$\begin{cases} \hat{X}_0 = \dfrac{\partial}{\partial\, t}, \qquad \hat{X}_1 = \dfrac{\partial}{\partial\, x}, \\ \hat{X}_2 = p\, \dfrac{\partial}{\partial\, p} + x\, \dfrac{\partial}{\partial\, x} - V\, \dfrac{\partial}{\partial\, V}. \end{cases} \tag{10}$$

Proof: Invariance with respect to one parameter groups generated by the operators $\hat{X}_0$, $\hat{X}_1$ is a direct consequence of the fact that system (9) does not depend explicitly on t and x. The operator $\hat{X}_2$ is the generator of scaling transformation

$$u' = u, \qquad p' = e^{\alpha}\, p, \qquad V' = e^{-\alpha}\, V, \qquad t' = t \qquad \text{and} \qquad x' = e^{\alpha}\, x.$$

Invariance of the system (9) with respect to this transformation is easily verified by direct substitution.

From the above symmetry generators one can take the following combination:

$$\hat{Z} = \frac{\partial}{\partial t} + \xi \left[(x - x_0) \frac{\partial}{\partial x} + p \frac{\partial}{\partial p} - V \frac{\partial}{\partial V} \right].$$

It is obvious that the operator $\hat{Z}$ belongs to the Lie algebra of the symmetry group of (9). Therefore expressing the old variables in terms of four independent solutions of equation $\hat{Z}\, J(t,\, x) = 0$, we gain the reduction of the initial system [12]. Solving the equivalent characteristic system

$$\frac{d\,t}{1} = \frac{d\,(x_0 - x)}{\xi (x_0 - x)} = \frac{d\,p}{\xi\,p} = \frac{d\,V}{-\xi\,V} = \frac{d\,u}{0},$$

we get the following ansatz, leading to the reduction:

$$u = U(\omega), \quad p = \Pi(\omega)\,(x_0 - x), \quad V = R(\omega)/(x_0 - x), \quad \omega = \xi\, t + \log \frac{x_0}{x_0 - x}. \tag{11}$$

In fact, inserting (11) into the second equation of (9), we get the quadrature

$$U = \xi R + \text{const}, \tag{12}$$

and the following dynamical system:

$$\begin{aligned} \xi\,\Delta(R) R' &= -R\,\left[\sigma R \Pi - \kappa + \tau \xi R \gamma\right] = F_1, \\ \xi\,\Delta(R)\Pi' &= \xi\,\left\{\xi R\,(R\Pi - \kappa) + \chi\,(\Pi + \gamma)\right\} = F_2, \end{aligned} \tag{13}$$

where $(\cdot)' = d\,(\cdot)\,/d\omega$, $\quad \Delta(R) = \tau(\xi R)^2 - \chi$, $\quad \sigma = 1 + \tau\xi$.

In case when $\gamma < 0$, the system (13) has three stationary points in the right half-plane. One of them, having the coordinates $R_0 = 0$, $\Pi_0 = -\gamma$, lies in the vertical coordinate axis. Another one having the coordinates $R_1 = -\kappa\,/\gamma$, $\Pi_1 = -\gamma$ is the only stationary point lying in the physical parameters range. The last one having the coordinates

$$R_2 = \sqrt{\frac{\chi}{\tau\xi^2}}, \qquad \Pi_2 = \frac{\kappa - \tau\xi\gamma R_2}{\sigma R_2},$$

lies on the line of singular points $\tau(\xi R)^2 - \chi = 0$.

As was announced earlier, we are looking for the homoclinic trajectory arising as a result of a limit cycle destruction. So in the first step we should assure the fulfillment of the Andronov–Hopf theorem statements in some stationary point. Since the only good candidate for this purpose is the point $A\,(R_1,\ \Pi_1)$, we put the origin into this point. Introducing new coordinates $X = R - R_1$, $Y = \Pi - \Pi_1$ we get the following system:

$$\xi\,\Delta(R)\begin{pmatrix} X \\ Y \end{pmatrix}' = \begin{bmatrix} -\kappa, & -R_1^2\sigma \\ \kappa\xi^2, & (\xi R_1)^2+\chi\xi \end{bmatrix}\begin{pmatrix} X \\ Y \end{pmatrix} + \begin{pmatrix} H_1 \\ H_2 \end{pmatrix}, \tag{14}$$

where

$$H_1 = -\left(\Pi_1 X^2 + 2\sigma R_1 XY + \sigma X^2 Y\right),$$
$$H_2 = \xi^2\left(\Pi_1 X^2 + 2R_1 XY + X^2 Y\right).$$

A necessary condition for appearance of the limit cycle reads as follows [13]:

$$\mathrm{sp}\,\hat{M} = 0 \;\Leftrightarrow\; (\xi R_1)^2 + \chi\xi = \kappa, \tag{15}$$

$$\det\hat{M} > 0 \;\Leftrightarrow\; \Omega^2 = \kappa\xi\,\Delta(R_1) > 0, \tag{16}$$

where $\hat{M}$ is the linearization matrix of system (14). The inequality (16) will be fulfilled if $\xi < 0$ and the coordinate R_1 lies inside the set $(0, \sqrt{\chi/(\tau\xi^2)})$. Note that another option, i.e. when $\xi > 0$ and $\Delta > 0$ is forbidden from physical reason [14]. In view of that, the critical value of ξ is expressed by the formula

$$\xi_{\rm cr} = -\frac{\chi + \sqrt{\chi^2 + 4\kappa R_1^2}}{2R_1^2}. \tag{17}$$

REMARK. Note that as a by-product of inequalities (15), (16) we get the relations

$$-1 < \tau\xi < 0. \tag{18}$$

To accomplish the study of the Andronov–Hopf bifurcation, we are going to calculate the real part of the first Floquet index C_1 [13]. For this purpose we use the transformation

$$y_1 = X, \qquad y_2 = -\frac{\kappa}{\Omega}X - \frac{\sigma R_1^2}{\Omega}Y, \tag{19}$$

enabling to pass from the system (14) to the canonical one having the following anti-diagonal linearization matrix

$$\hat{M}_{ij} = \Omega(\delta_{2i}\delta_{1j} - \delta_{1i}\delta_{2j}).$$

For this the representation formulae from [13, 15] are directly applied and using them we obtain the expression

$$16\,R_1^2\,\Omega^2\,\mathrm{Re}\;\;C_1 = -\kappa\,\left\{3\kappa^2 + (\xi\,R_1)^2\,(3-\xi\,\tau) - \kappa\,(\xi\,R_1)^2\,(6+\tau\,\xi)\right\}.$$

Employing (15), we get, after some algebraic manipulation, the formula

$$\mathrm{Re}\;\;C_1 = \frac{\kappa}{16\,\Omega^2\,R_1^2}\left\{2\kappa\,\xi\,\tau\,(\xi\,R_1)^2 - \chi\,\tau\,\left(\xi^2 R_1\right)^2 - 3\,(\chi\,\xi)^2\right\}.$$

Since for $\xi = \xi_{\rm cr} < 0$ the expression in braces is negative, the following statement is true:

LEMMA 2. *If* $R_1 < R_2$ *then in vicinity of the critical value* $\xi = \xi_{cr}$ *given by formula* (17) *a stable limit cycle appears in the system* (13).

We have formulated conditions assuring the appearance of periodic orbit in the vivinity of stationary point $A(R_1,\ \Pi_1)$. Yet, in order that the required homoclinic bifurcation would ever take place, another condition should be fulfilled, namely that, with the same restrictions upon the parameters, the critical point $B(R_2,\ \Pi_2)$ is a saddle. Besides, it is necessary to pose the conditions on the parameters assuring that the stationary point $B(R_2,\ \Pi_2)$ lies in the first quadrant of the phase plane. Otherwise the corresponding stationary solution which is needed to compose the compacton would not have any physical interpretation. Below we formulate the statement addressing both of these questions.

LEMMA 3. *The stationary point* $B(R_2,\ \Pi_2)$ *is a saddle lying in the first quadrant for any* $\xi > \xi_{cr}$ *if the following inequalities hold:*

$$-\tau\,\xi_{cr}\,R_2 < R_1 < R_2. \tag{20}$$

Proof: First we are going to show that the eigenvalues $\lambda_{1,2}$ of the Jacobi matrix of (13)

$$\hat{M} = \frac{\partial\,(F_1,\ F_2)}{\partial\,(R,\ \Pi)}\bigg|_{R_2,\,\Pi_2} = \begin{bmatrix} \kappa, & \dfrac{\sigma\,\chi}{\tau\,\xi^2} \\ \dfrac{\xi^2\,[\kappa(\sigma-2)+2\gamma\,R_2(\sigma-1)]}{\sigma}, & -\dfrac{\chi\sigma}{\tau} \end{bmatrix} \tag{21}$$

are real and have different signs. Since the eigenvalues of $\hat{M}$ are expressed by the formula

$$\lambda_{1,2} = \frac{\mathrm{sp}\ \hat{M} \pm \sqrt{\left[\mathrm{sp}\ \hat{M}\right]^2 - 4\,\det\hat{M}}}{2},$$

it is sufficient to show that

$$\det\hat{M} < 0. \tag{22}$$

In fact, we have

$$\begin{aligned}\det\hat{M} &= -\frac{\chi\,\sigma\,\kappa}{\tau} - \frac{\chi}{\tau}\,[\kappa\,(\sigma-2)+2\,\gamma\,R_2\,(\sigma-1)] \\ &= -\frac{\chi}{\tau}2\,\gamma\,\tau\,\xi\left(\frac{\kappa}{\gamma}+R_2\right) = 2\,\chi\,\xi\,\gamma\ (R_1-R_2) < 0.\end{aligned}$$

To finish the proof, we must show that the stationary point $B(R_2,\ \Pi_2)$ lies in the first quadrant. This is equivalent to the statement that

$$\kappa - \tau\,\xi_{cr}\,\gamma\,R_2 > 0.$$

Dividing the inequality obtained by $\gamma < 0$ and moving the first term into the RHS, we get the inequality $-\tau\,\xi_{cr}\,R_2 < R_1$. The latter implies inequalities $-\tau\,\xi\,R_2 < R_1 < R_2$ which are valid for any $\xi > \xi_{cr}$. This ends the proof.

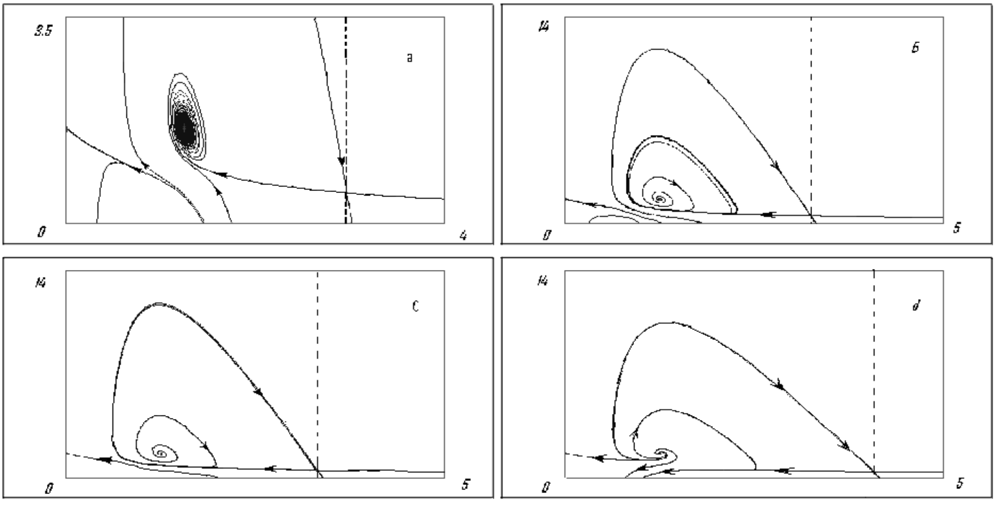

Fig. 3. Changes of the phase portrait of system (13): (a) $A(R_1,\ \Pi_1)$ is the stable focus; (b) $A(R_1,\ \Pi_1)$ is surrounded by the stable limit cycle; (c) $A(R_1,\ \Pi_1)$ is surrounded by the homoclinic loop; (d) $A(R_1,\ \Pi_1)$ is the unstable focus;

Numerical studies of the behavior of (13) reveal the following changes of regimes (cf. Fig. 3). When $\xi < \xi_{\rm cr}$, $A(R_1, \Pi_1)$ is a stable focus; above the critical value a stable limit cycle softly appears. Its radius grows with the growth of the parameter ξ until it gains the second critical value $\xi_{{\rm cr}_2} > \xi_{\rm cr}$ for which the homoclinic loop appears in place of the periodic trajectory. The homoclinic trajectory is based upon the stationary point $B(R_2, \Pi_2)$ lying on the line of singular points $\Delta(R) = 0$, so it corresponds to the generalized compacton-like solution to system (9). We obtain this solution sewing up the TW solution corresponding to homoclinic loop with stationary inhomogeneous solution

$$u = 0, \qquad p = \Pi_2\,(x_0 - x), \qquad V = R_2/(x_0 - x), \tag{23}$$

corresponding to critical point $B(R_2, \Pi_2)$. So, strictly speaking it is different from the "true" compacton, which is defined as a solution with compact support. Note that we can pass to the compactly supported function by the following change of variables:

$$\pi(t,\ x) = p(t, x) - \Pi_2\,(x_0 - x), \qquad \nu(t,\ x) = V(t, x) - R_2/(x_0 - x).$$

4. Numerical investigations of system (9)

4.1. Construction and verification of the numerical scheme.

We construct the numerical scheme basing on the S. K. Godunov method [16, 17]. Let us consider the calculating cell $a\,b\,c\,d$ (see Fig. 4) lying between $n - th$ and

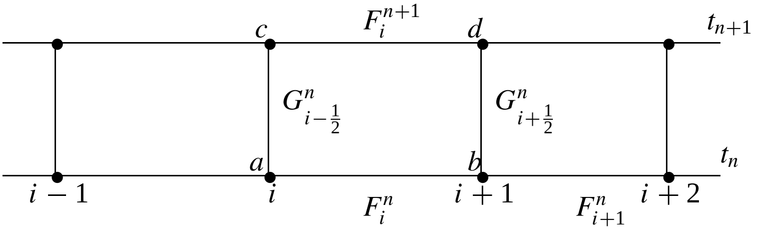

Fig. 4. Scheme of calculating cells

$(n+1)-th$ temporal layers of the uniform rectangular mesh. It is easy to see that system (9) can be presented in the following vector form,

$$\frac{\partial F}{\partial t} + \frac{\partial G}{\partial x} = H, \tag{24}$$

with $F = (u,\, V,\, p - \chi/V)^{\mathrm{tr}}$, $G = (p,\, -u,\, 0)^{\mathrm{tr}}$ and $H = (\gamma,\, 0,\, \kappa/V - p)^{\mathrm{tr}}$ where $(\cdot)^{\mathrm{tr}}$ stands for the operation of transposition. From (24) arises the equality of integrals

$$\int\int_\Omega \left(\frac{\partial F}{\partial t} + \frac{\partial G}{\partial x}\right) dx\, dt = \int\int_\Omega H\, dx\, dt,$$

where Ω is identified with the rectangle $a\,b\,c\,d$. Due to the Gauss–Ostrogradsky theorem, integral in the LHS of the above equation can be presented in the form

$$\int\int_\Omega \left(\frac{\partial F}{\partial t} + \frac{\partial G}{\partial x}\right) dx\, dt = \oint_{\partial\Omega} G\, d\,t - F\, d\,x. \tag{25}$$

Let us denote the distance between the $i-th$ and $(i+1)-th$ nodes of the OX axis by $\Delta\, x$ while the corresponding distance between the temporal layers by $\Delta\, t$. Then, up to $O\left(|\Delta\, x|^2,\ |\Delta\, t|^2\right)$, we get from equations (24), (25) the following difference scheme,

$$\left(F_i^{n+1} - F_i^n\right)\, \Delta\, x + \left(G^{n+1}_{i+\frac{1}{2}} - G^n_{i-\frac{1}{2}}\right)\, \Delta\, t = H_i^n \Delta\, x\, \Delta\, x, \tag{26}$$

where $G^{n+1}_{i+\frac{1}{2}}$, $G^{n+1}_{i-\frac{1}{2}}$ are the values of the vector function G on the segments $b\,c$ and $a\,d$, correspondingly. In the Godunov method these values are defined by solving the Riemann problem. Below we describe the procedure of their calculation.

According to the common practice [18], instead of dealing with the initial system (9), we look for the solution of the Riemann problem $(u_1,\ V_1,\ p_1)$ at $x < 0$ and $(u_2,\ V_2,\ p_2)$ at $x > 0$ to the corresponding homogeneous system

$$\begin{aligned} u_t + p_x &= 0, \\ V_t - u_x &= 0, \\ p_t + \frac{\chi}{\tau V^2} V_t &= 0. \end{aligned} \tag{27}$$

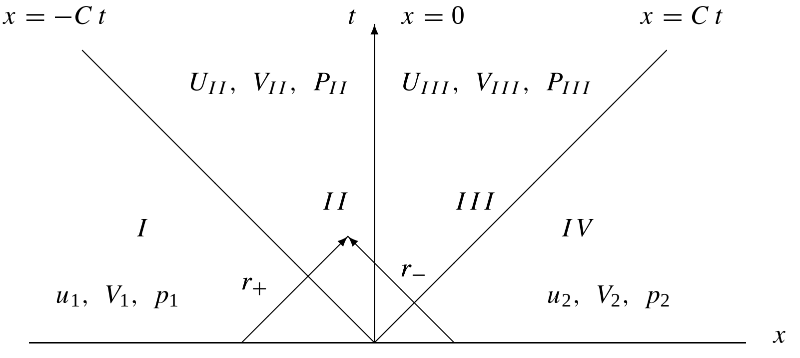

Fig. 5. Scheme of solving the Riemann problem.

It is easy to see that linearisation of the system (27) has three characteristic velocities: $C_0 = 0$ and $C_\pm = \pm C \equiv \pm\sqrt{\frac{\chi}{\tau V_0^2}}$, where $V_0 = \frac{V_1+V_2}{2}$. The Riemann invariants corresponding to them are as follows (we calculate them in the acoustic approximation):

$$r_0 = p - \frac{\chi}{\tau V}, \qquad r_\pm = p \pm C\,u.$$

The characteristics $x = \pm C\,t$ and $x = 0$ divide the half-plane $t \geq 0$ into four sectors (see Fig. 5) and the problem is to find the values of the parameters in sectors II and III, basing on the values $(u_1,\ V_1,\ p_1)$ and $(u_2,\ V_2,\ p_2)$ which are assumed to be defined. The scheme of calculating the values $U_{II},\ P_{II}$ is based on the property of the Riemann invariants to retain their values along the corresponding characteristics. From this we get the system of algebraic equations (cf. with Fig. 5):

$$p_1 + C\,u_1 = P_{II} + C\,U_{II},$$
$$p_2 - C\,u_2 = P_{II} - C\,U_{II}.$$

The system of determining equations for $U_{III},\ P_{III}$ occurs to be the same, so the values of the parameters U, P in the sector $-Ct < x < Ct$, $C = \sqrt{\chi/(\tau V_0^2)}$ are given by the formulae:

$$U = \frac{u_1 + u_2}{2} + \frac{p_1 - p_2}{2C}, \tag{28}$$
$$P = \frac{p_1 + p_2}{2} + C\frac{u_1 - u_2}{2}.$$

Expression for the function V is omitted since it does not take part in the construction of the scheme of this stage.

With some additional assumption the Riemann problem can be solved without resorting to the acoustic approximation. Let us assume that

$$p = \frac{\chi}{\tau V}. \tag{29}$$

As is easily seen, this relation is the particular integral of the third equation of the system (27). Employing this formula, we can write down the first two equations as the following closed system:

$$\left(\frac{\partial}{\partial t} + \tilde{A}\frac{\partial}{\partial x}\right)\begin{pmatrix} u \\ V \end{pmatrix} = 0, \quad \text{where} \quad \tilde{A} = \begin{pmatrix} 0, & -\chi/(\tau V^2) \\ -1, & 0 \end{pmatrix}. \tag{30}$$

Solving the eigenvalue problem $\det||\tilde{A} - \lambda I|| = 0$, we find that the characteristic velocities satisfy the equation

$$\lambda^2 = C_{L\infty}^2 = \chi/(\tau V^2).$$

Now we look for the Riemann invariants in the form of infinite series

$$r_{\pm} = V \sum_{\nu=0}^{\infty} A_{\nu}^{\pm} u^{\nu}.$$

It is not difficult to verify by direct inspection that the following relations hold:

$$D_{\pm}V = \left(\frac{\partial}{\partial t} \pm C_{L\infty}\frac{\partial}{\partial x}\right) V = u_x \pm C_{L\infty} V_x = Q_{\pm}, \tag{31}$$

$$D_{\pm}u = \pm C_{L\infty} Q_{\pm}. \tag{32}$$

Using (32) and (32), we find the recurrent formula

$$A_n^{\pm} = (\mp 1)^n \frac{A_0}{n!(\sqrt{\chi/\tau})^n}.$$

and finally obtain the expression for Riemann invariants:

$$r^{\pm} = A_0 V \exp\ (\mp u/\sqrt{\chi/\tau}). \tag{33}$$

So under the assumption that $p = \frac{\chi}{\tau V}$, the system (27) can be rewritten in the form

$$D_{\pm} r^{\pm} = 0. \tag{34}$$

Using (29) and (34) we get the solution of the Riemann problem in the sector $\sqrt{\chi/(\tau V_1^2)}t < x < \sqrt{\chi/(\tau V_2^2)}t$:

$$U = \sqrt{\chi/\tau}\ \ ln\ \ Z, \tag{35}$$

$$P = p_2 + \sqrt{\chi/\tau} C_2 [Z \exp(-u_2/\sqrt{\chi/\tau}) - 1],$$

where

$$Z = (E + \sqrt{Q})/(2C_2\sqrt{\chi/\tau}),$$

$$E = \exp(u_2/\sqrt{\chi/\tau})\{p_1 - p_2 + \sqrt{\chi/\tau}(C_2 - C_1)\},$$

$$Q = E^2 + 4\chi/\tau C_1 C_2 \exp[(u_1 + u_2)/\sqrt{\chi/\tau}],$$

$$C_i = \sqrt{\chi/\tau}/V_i \equiv C_{L\infty}(V_i), \quad i = 1, 2.$$

Note that (35) is reduced to (28) when $|p_1 - p_2| << 1$, $|u_1 - u_2| << 1$.

Thus, the difference scheme for (9) takes the following form:

$$(u_i^n - u_i^{n+1})\Delta x - (p_{i+1/2}^n - p_{i-1/2}^n)\Delta t = -\gamma \Delta t \Delta x,$$

$$(V_i^n - V_i^{n+1})\Delta x + (u_{i+1/2}^n - u_{i-1/2}^n)\Delta t = 0,$$

$$\left(p_i^n - \frac{\chi}{\tau V_i^n}\right)\Delta x - \left(p_i^{n+1} - \frac{\chi}{\tau V_i^{n+1}}\right)\Delta x = -f \Delta t \Delta x,$$

where $(u_{i-1/2}^n, p_{i-1/2}^n)$ and $(u_{i+1/2}^n, p_{i+1/2}^n)$ are solutions of Riemann problems $(V_{i-1}^n, u_{i-1}^n, p_{i-1}^n)$, (V_i^n, u_i^n, p_i^n) (V_i^n, u_i^n, p_i^n), $(V_{i+1}^n, u_{i+1}^n, p_{i+1}^n)$, correspondingly,

$$f = f(p_i^k, V_i^k) = \frac{\kappa}{V_i^k} - p_i^k,$$

k is equal to either n or $n+1$. The choice $k = n$ leads to the explicit Godunov scheme

$$\begin{cases} u_i^{n+1} = u_i^n + \dfrac{\Delta t}{\Delta x}\left(p_{i-1/2}^n - p_{i+1/2}^n\right) + \gamma \Delta t, \\ V_i^{n+1} = V_i^n + \dfrac{\Delta t}{\Delta x}(u_{i+1/2}^n - u_{i-1/2}^n), \\ p_i^{n+1} = p_i^n + \dfrac{\chi}{\tau}\left(\dfrac{1}{V_i^{n+1}} - \dfrac{1}{V_i^n}\right) + f(p_i^n, V_i^n)\Delta t. \end{cases} \tag{36}$$

The scheme (36) was tested on invariant TV solutions of the form:

$$u = U(\omega), \qquad p = P(\omega), \qquad V = V(\omega), \qquad \omega = x - Dt. \tag{37}$$

Inserting (37) into first two equations of system (9), one can obtain the following first integrals:

$$\begin{cases} U = u_1 + D(V_1 - V), \\ P = p_1 + D^2(V_1 - V), \end{cases} \tag{38}$$

where $V_1 = \lim_{\omega\to\infty} V(\omega)$. Let us assume in addition that $u_1 = 0$, while $p_1 = \kappa/V_1$. With this assumption the constants (u_1, p_1, V_1) satisfy the initial system.

Inserting U and P into the third equation of (9) we get

$$\frac{dV}{d\omega} = -V\frac{[D^2V^2 - SV + \kappa]}{\tau D[C_{T\infty}^2 - (DV)^2]} = F(V), \tag{39}$$

where $C_{T\infty} = \sqrt{\chi/\tau}$, $S = p_1 + D^2V_1$. Eq. (39) has three critical points:

$$V = V_0 = 0, \qquad V = V_1, \qquad V = V_2 = \kappa/(V_1D^2).$$

If the inequality $V_2 = \kappa/(V_1D^2) < V_1$ holds and the line $\chi/\tau - (DV)^2 = 0$ is outside the interval (V_2, V_1), then the constants

$$u_{-\infty} = u_2 = \frac{(DV_1)^2 - \kappa}{DV_1} > 0, \qquad p_{-\infty} = p_2 = \kappa/V_2, \qquad V_{-\infty} = V_2,$$

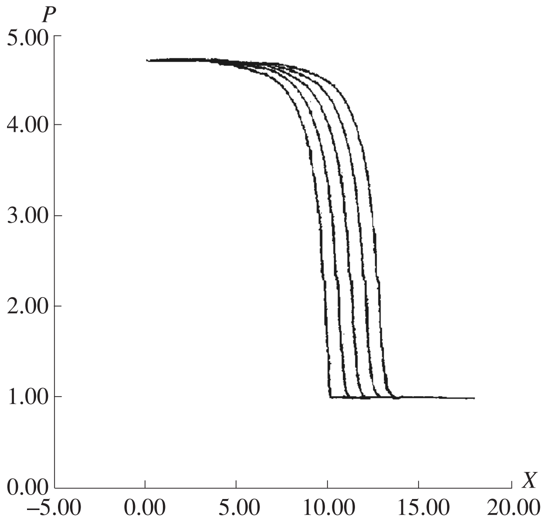

Fig. 6. Temporal evolution of Cauchy data defined by solutions of Eq. (39) and the first integrals (38). The following values of the parameters were chosen during numerical simulation: $\kappa = 0.5$, $\chi = 0.25$, $\tau = 0.1$, $V_1 = 0.5$, $D = 3.1$.

deliver the second stationary solution to the initial system and solution of equation (39) corresponds to a smooth compressive wave connecting stationary points V_2 and V_1.

Results of numerical solution of the Cauchy problem based on the Godunov scheme (36) are shown in Fig. 6. As the Cauchy data we took the smooth self-similar solution obtained by numerical solution of Eq. (39) and the use of the first integrals (38). So we see that the numerical scheme describes quite well the self-similar evolution of the initial data.

4.2. Numerical investigations of the temporal evolution and attractive features of compactons.

Below we present the results of numerical solution of the Cauchy problem for system (9). In numerical experiments we used the values of the parameters taken in accordance with the preliminary results of qualitative investigations and corresponding to the homoclinic loop appearance in system (13). As the Cauchy data we got the generalized solution describing the compacton and obtained by the preliminary solurion of (13) and using the formulae (12), (23). Results of the numerical simulation are shown in Fig. 7. It is seen that compacton evolves for a long time in a stable self-similar mode.

Additionally the numerical experiments revealed that the wave packets are created by sufficiently wide family of initial data tend, under certain conditions, to the compacton solution. The following family of initial perturbations have been considered

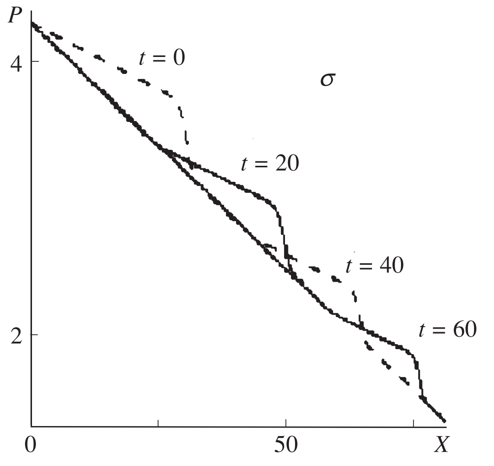

Fig. 7. Numerical solution of the system (9) in case when the invariant homoclinic solution is taken as the Cauchy data.

in the numerical experiments:

$$p = \begin{cases} p_0(x_0 - x) & \text{when } x \in (0, a) \cup (a + l, x_0) \\ (p_0 + p_1)(x_0 - x) + w(x - a) + h & \text{when } x \in (a, a + l), \\ u = 0, \quad V = \kappa/p. \end{cases} \tag{40}$$

Here a, l, p_1, w, h are parameters of the perturbation defined on the background of the inhomogeneous stationary solution (23). Note that l defines the width of the initial perturbation. Varying broadly parameters of the initial perturbation, in numerical experiments we observed that, when fixing e.g. the value of l, it was possible to fit in many ways the rest of parameters such that one of the wave packs created by the perturbation (namely that one which runs “downwards” in the direction of diminishing pressure) in the long run approaches the compacton solution. Whether the wave pack would approach the compacton solution or not depends on that part of energy of the initial perturbation which is carried out “downwards”. Assuming that the energy is divided between two wave packs created more or less in half, we can use for the rough estimation of convergency the total energy of the initial perturbation, consisting of the internal energy E_{int} and the potential energy E_{pot}:

$$E = E_{\text{int}} + E_{\text{pot}} = \int \left[\varepsilon_{\text{int}} + \varepsilon_{\text{pot}}\right] dx,$$

where ε_{int}, and ε_{pot} are local densities of the corresponding terms

The function ε_{pot} is connected with forces acting in the system by means of the evident relation

$$\gamma - \frac{1}{\rho}\frac{\partial p}{\partial x_e} = -\frac{\partial \varepsilon_{\text{pot}}}{\partial x_e},$$

where x_e is the physical (Eulerian) coordinate connected with the mass Lagrangean coordinate x as

$$x = \int V^{-1} \, d\, x_e.$$

From this we extract the expression

$$E_{\text{pot}} = \int \varepsilon_{pot} \, d\, x = \int_{\Omega} \left[\int_{c_1}^{x_e} \left(V \frac{\partial p}{\partial x_e} - \gamma \right) dx_e' \right] V^{-1} dx_e,$$

where Ω is the support of initial perturbation.Employing in the above integral the relation $V\, \partial p / \partial x_e = \partial p / \partial x$, we obtain

$$E_{\text{pot}} = \frac{\kappa\, l}{\alpha + \beta} \left[\left(\frac{1+k}{k} \right) \ln(1 + k) - 1 \right],$$

where $k = [P\,(a + l) - P\,(a)]/P\,(a)$, $P(z) = \alpha z + \beta$, $\alpha = w - (p_0 + p_1)$, $\beta = (p_1 + p_0) x_0 - a w$.

For $\chi = 1.5$, $\kappa = 10$, $\gamma = -0.04$, $\tau = 0.07$, $x_0 = 120$, convergency was observed when E_{tot} was close to 45 (see Figures below).

The function ε_{int} is obtained from the second low of thermodynamics written for the adiabatic case: $(\partial \varepsilon_{\text{int}} / \partial V)_S = -p = -\kappa / V$. From this we get

$$\varepsilon_{\text{int}} = c - \kappa \ln V.$$

To obtain the energy of perturbation itself, we should subtract from this value the energy density of stationary inhomogeneous solution $c - \kappa \ln V_0$, so finally we get

$$E_{\text{int}} = \int_{\Omega} (\varepsilon_{\text{int}} - \varepsilon_{\text{int}}^0) V^{-1} dx_e = \kappa \int_{\Omega} \ln V_0 / V \, dx_l.$$

Using the formula (40),we finally obtain

$$E_{\text{int}} = \kappa \left\{ l \ln \frac{P(a + l)}{P_0(a + l)} + \frac{P(a)}{\alpha} \ln \left[1 + \frac{\alpha l}{P(a)} \right] + \frac{P_0(a)}{p_2} \ln \left[1 - \frac{p_2 l}{P_0(a)} \right] \right\},$$

where $P_0(z) = p_0(x_0 - z)$.

Numerical experiment shows that the energy norm serves as sufficiently good criterion of convergency. At $\chi = 1.5$, $\kappa = 10$, $\gamma = -0.04$, $\tau = 0.07$, $x_0 = 120$ convergency was observed when $E \in (43, 47)$. The patterns of evolution of the wave perturbations are shown in Fig 8. For comparison we also show the temporal evolution of the wave packs created by the perturbations for which $E \notin (43,\ 47)$ (Fig. 9).

Thus there is observed some correlation between the energy of initial perturbation and convergency of the created wave packets to the compacton solution.

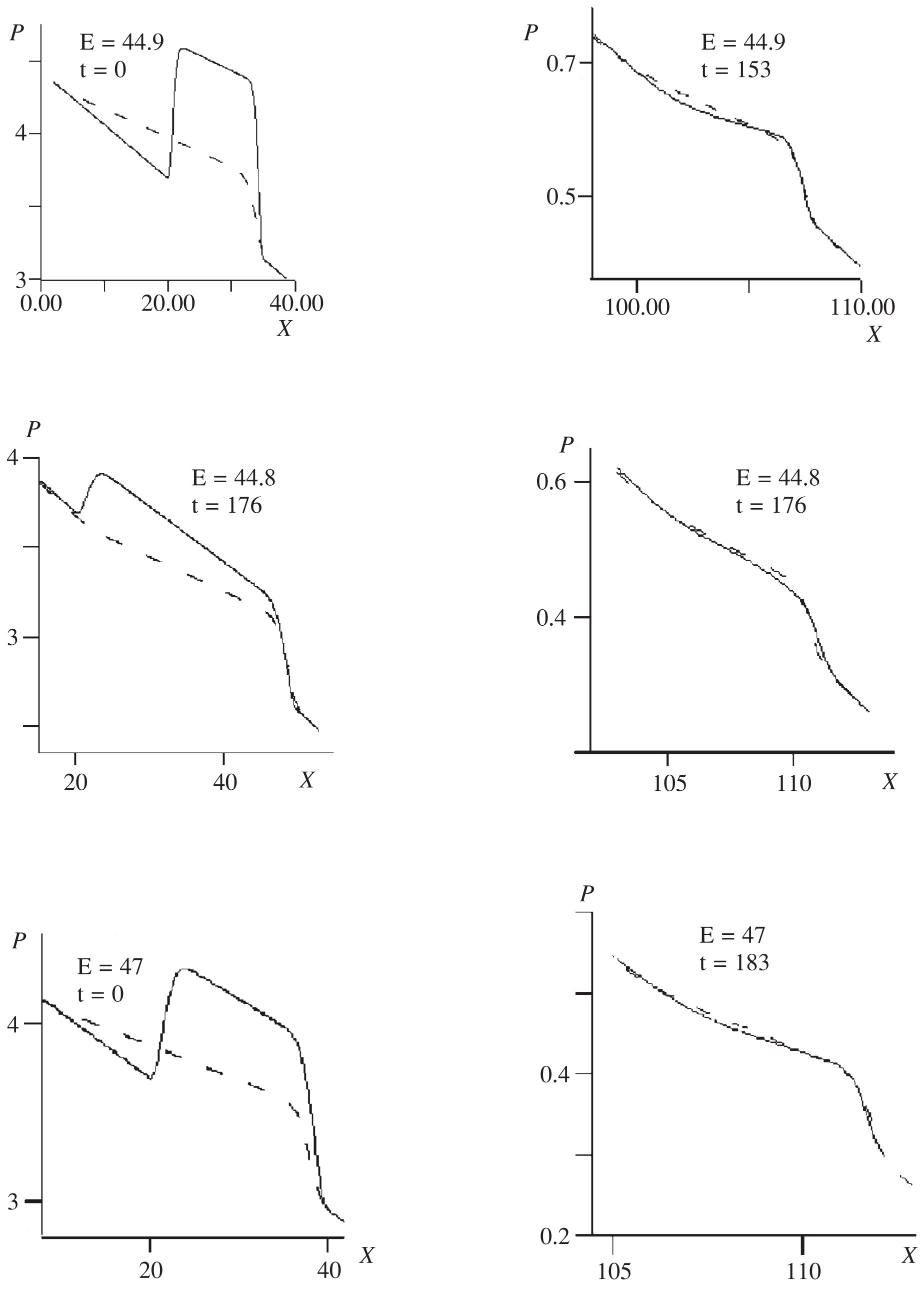

Fig. 8. Perturbations of ??stationary invariant solutions of system (9) (left) and TW solutions created by these perturbations (right) on the background of the invariant compacton-like solution (dashed).

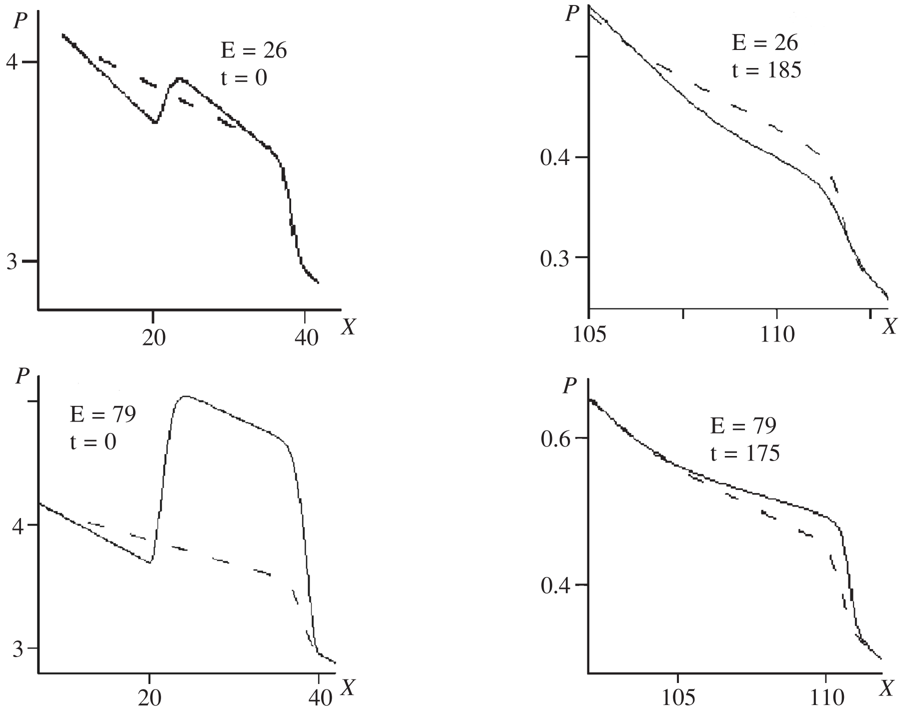

Fig. 9. Evolution of the wave patterns created by the local perturbations which do not satisfy the energy criterion.

5. Conclusions and discussion

In this work we have discussed the origin of generalized TW solutions called compactons and have shown the existence of such solutions within the hydrodynamic-type model of relaxing media. The main results concerning this subject can be summarized as follows:

- The family of TW solutions to (9), given by the formula (11), includes a compacton in *case when an external force is present (more precisely, when* $\gamma < 0$*).*
- Compacton solution to system (9) occurs merely at selected values of the parameters: *for fixed* κ, γ *and* χ *there is a unique compacton-like solution, corresponding to the value* $\xi = \xi_{cr_2}$.

Qualitative numerical analysis of the corresponding ODE system describing the TW solutions to the initial system served us as a starting point in numerical investigations of compactons, based on the Godunov method. Numerical investigations reveal that compacton encountered in this particular model form a stable wave pattern evolving in a self-similar mode. It was also obtained a numerical evidence of attracting features of this structure: a wide class of initial perturbations creates wave packs tending to compacton. Convergency only weakly depends on the shape of initial perturbation and is mainly caused by fulfillment of the energy criterion. Unfortunately, this criterion is not enough precise. In fact, it is not sensible to the form of initial perturbation, which, in turn, influences the part of the total energy getting away by the wave pack moving “downwards”. Besides, the Godunov scheme does not enable to obtain more strict quantitative measure of convergency. But in spite of these discrepancies the effect of convergency is evidently observed and this will be the topic of our further study to develop more strict criteria of convergency as well as to try to realize whether the compacton solution serves as true or intermediate [19, 20] asymptotics.

REFERENCES

[1] Y. A. Demekhin, G. Yu Tokarev and V. Ya. Shkadov: Hierarchy of Bifurcations of Space-Periodic Structures in Nonlinear Model of Active Dissipative Media, *Physica D* **52** (1991), 338–361.

[2] A. S. Davydov: Solitons and Energy Transfer Along Protein Molecules, *J. Theoret. Biology* **66** (1977), 379–387.

[3] R. I. Soloukhin: Detonation Waves in Gaseous Media, *Uspekhi Fizicheskich Nauk*, vol, LXXX (1963), No 4, 525–551 (in Russian).

[4] F. Zhang and H. Gronig: Spin Detonation in Reactive Particles-Oxidizing Gas Flow, *Phys. of Fluids A: Fluid Dynamics* **3** (1991), no 8, 1983–1990.

[5] R. K. Dodd, J. C. Eilbek, J. D. Gibbon and H. C. Morris: Solitons and Nonlinear Wave Equations, Academic Press, London 1984.

[6] P. Rosenau and J. Hyman: Compactons: Solitons with Finite Wavelength, *Phys Rev. Letter* **70** (1993), No 5, 564–567.

[7] P. J. Olver and P. Rosenau: Tri-Hamiltonian duality between solitons and solitary-wave solutions having compact support, *Phys. Rev. E* **53** (1995), no 2, 1900–1906.

[8] Y. A. Li and P. J. Olver: *Convergence of Solitary-Wave Solutions in a Perturbed Bi-Hamiltonian Dynamical System. 1. Compactons and Peakons*, http://www.math.umn.edu/ olver

[9] P. Rosenau: On solitons, compactons and Lagrange maps, *Physics Letters A* **211** (1996), 265–275.

[10] V. A. Vakhnenko and V. V. Kulich: Long-wave processes in a periodic medium, *Journ. Appl. Mech. and Tech. Physics* (PMTF), **33**, no. 6 (1992), 814–820.

[11] V. A. Danylenko, V. V. Sorokina and V. A. Vladimirov: *On the governing equations in relaxing media models and self-similar quasiperiodic solutions*, *J. Phys. A* **26** (1993), 7125–7135.

[12] P. Olver: *Applications of Lie groups to Differential Equations*, Springer: New York, Berin, Tokyo 1996.

[13] B. Hassard, N. Kazarinoff and Y.-H. Wan: *Theory and Applications of Hopf Bifurcation*, Cambridge Univ. Press: London, New York 1981.

[14] L. D. Landau and E. M. Lifshitz: *Hydrodynamics*, Nauka Publ., Moscow 1984.

[15] J. Guckenheimer and P. Holmes: *Nonlinear Oscillations, Dynamical Systems and Bifurcations of Vector Fields*, Springer, New York Inc. 1987.

[16] S. K. Godunov: A Difference Scheme for Numerical Solution of Discontinuos Solution of Hydrodynamic Equations, *Math. Sbornik* **47** (1959), 271–306, translated *US Joint Publ. Res. Service*, JPRS 7226, 1969.

[17] B. L. Rozhdestvenskij and N. N. Yanenko: *Systems of Quasilinear Equations and Their Applications to Gas Dynamics*, Translations of Mathematical Monographs, 55, Providence, R.I: American Mathematical Society, vol. XX, 1983.

[18] A. M. Iskol'dskii, and E. I. Romenskii: A dynamic model of a thermoelastic continuous medium with pressure relaxation, *Journ. Appl. Mech. and Tech. Physics* (PMTF) **25**, no. 2 (1984), 286–291.
[19] G. I. Barenblatt: *Similarity, Self-Similarity and Intermediate Asymptotics*, Cambridge Univ. Press 1986.
[20] P. Blier and G. Karch (eds.): *Self-Similar Solutions in Nonlinear PDEs*, Banach Center Publications, **74**, Warsaw 2006.